Electronic Supplementary Material (ESI) for RSC Advances.

Supporting information

Aqueous electrostatic dispersion and heterocoagulation of multiwalled carbon nanotubes and manganese dioxide for the fabrication of supercapacitor electrodes and devices

Y.Liu and I.Zhitomirsky

Department of Materials Science and Engineering
McMaster University
1280 Main Street West
Hamilton, Ontario, Canada
L8S 4L7

*E-mail: zhitom@mcmaster.ca
Phone: 1- (905) 525 – 9140

Materials and fabrication of activated carbon –carbon black electrodes.

Trans-cinnamic acid (TCA), p-coumaric acid (PCA), and 2,4-dihydroxycinnamic acid (DCA) were purchased from Aldrich.

Activated carbon (AC) (PICACTIF, PICA) with specific area of 2300 m^2 g^{-1} and carbon black (CB) (Cabot) were used for the fabrication of electrodes. CB was used as a conductive additive. Poly(vinylidene flouride) (PVDF) binder and 1-Methyl-2-pyrrolidinone (MP) solvent were purchased from Alfa Aesar. Ni foams (95% porosity, Vale) were used as current collectors. The Ni foams were impregnated using slurries, containing AC, CB and PVDF in MP, and then dried at 70ºC in air for 4 h.

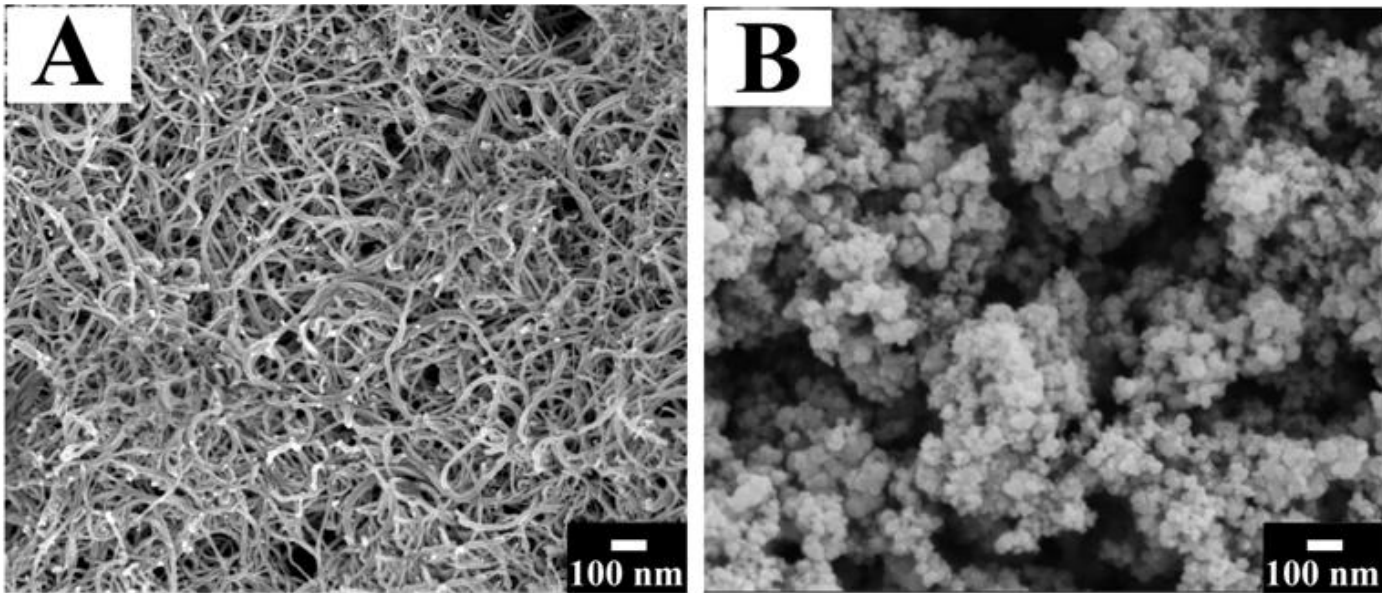

Figure S1. SEM images of (A) MWCNT, (B) MnO_2, deposited by EPD.

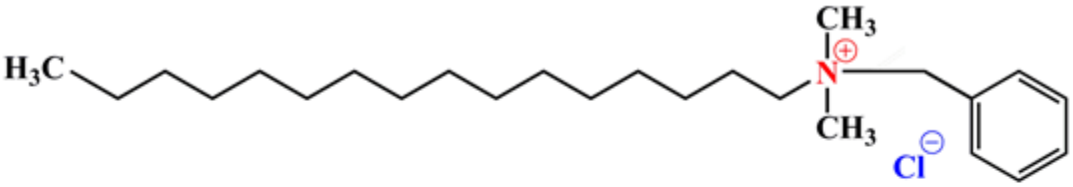

Benzyldimethylhexadecylammonium chloride (BAC)

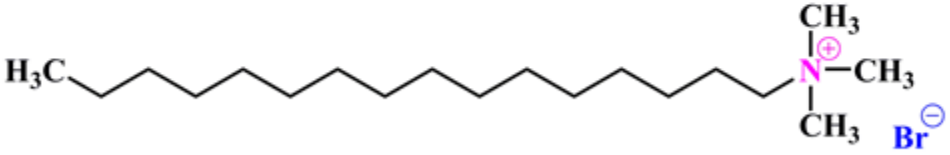

Hexadecyltrimethylammonium bromide (CTAB)

Figure S2. Comparison of chemical structures of benzyldimethylhexadecylammonium chloride (BAC) and hexadecyltrimethylammonium bromide (CTAB).

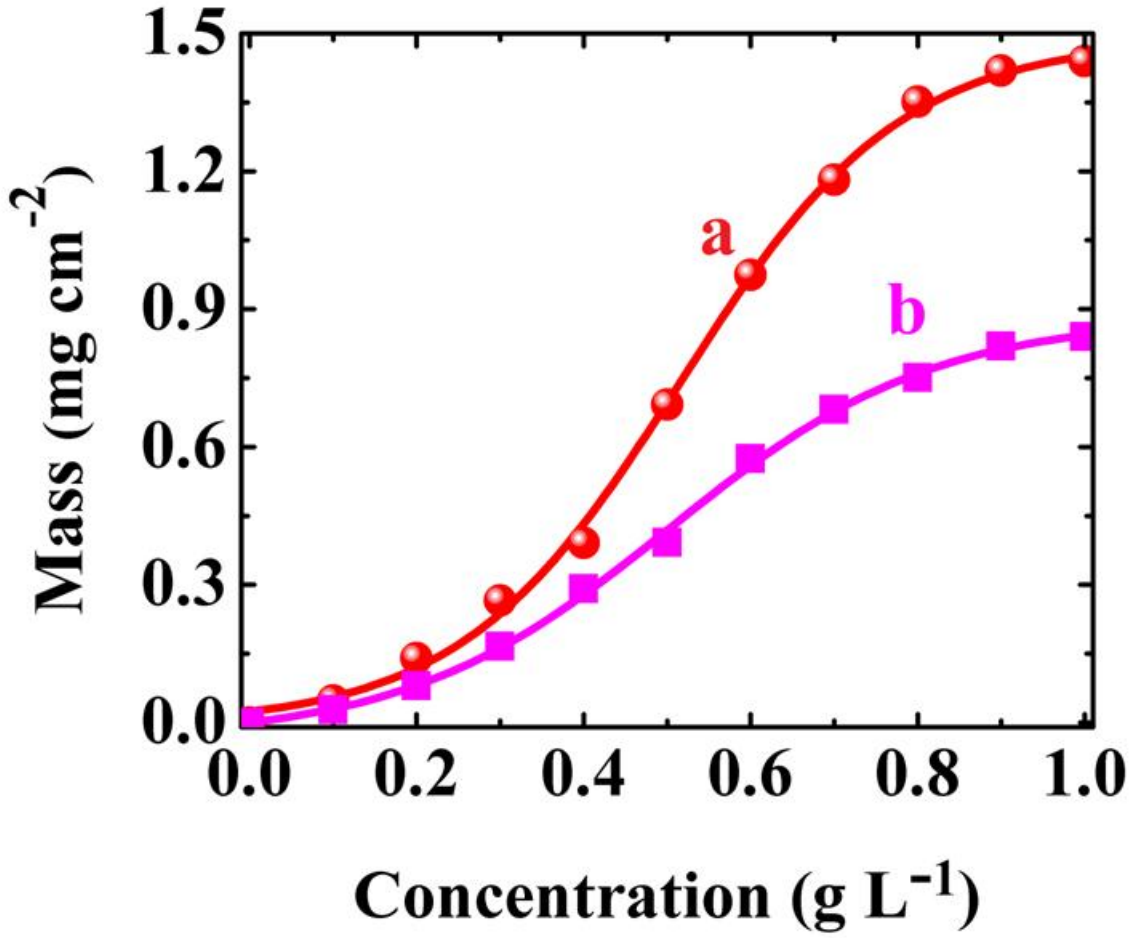

Figure S3. Comparison of the deposition yield obtained from 1 g L^{-1} MWCNT suspension in water at a deposition voltage of 20 V and deposition time of 3 min: (a) versus BAC concentration and (b) versus CTAB concentration.

A

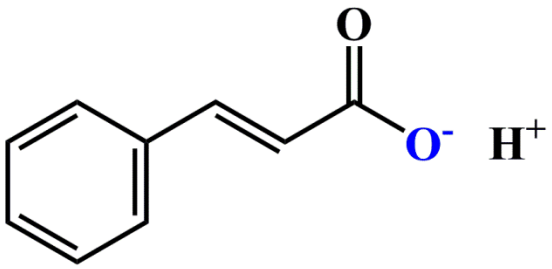

trans-cinnamic acid (TCA)

B

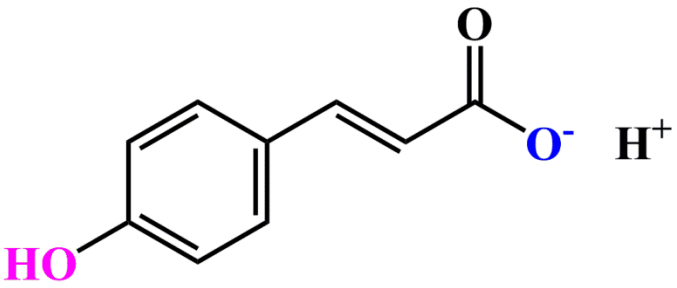

p-coumaric acid (PCA)

C

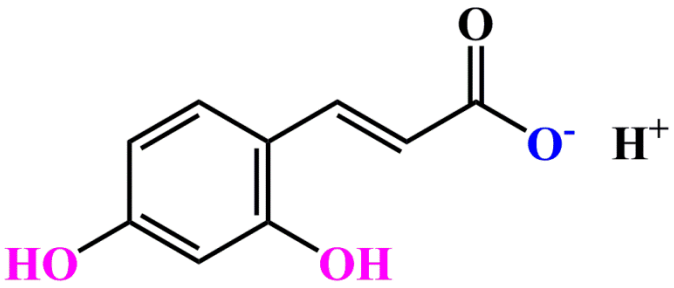

2,4-dihydroxycinnamic acid (DCA)

Figure S4. Chemical structures of (A) TCA, (B) PCA and (C) DCA

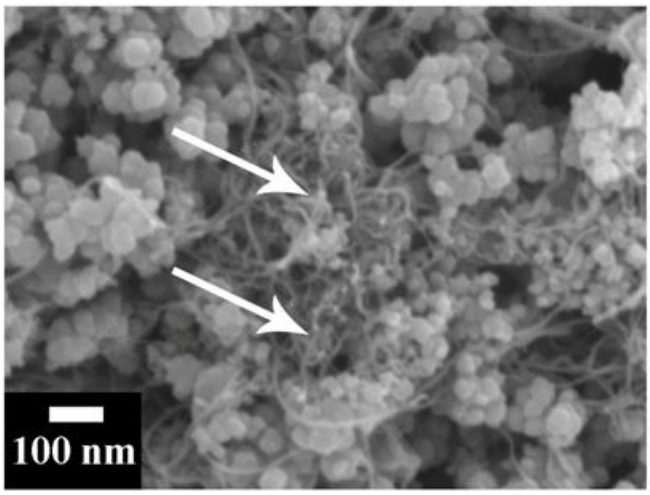

Figure S5. SEM image of MnO_2-MWCNT composite, prepared without dispersants. Arrows show MWCNT agglomerate.

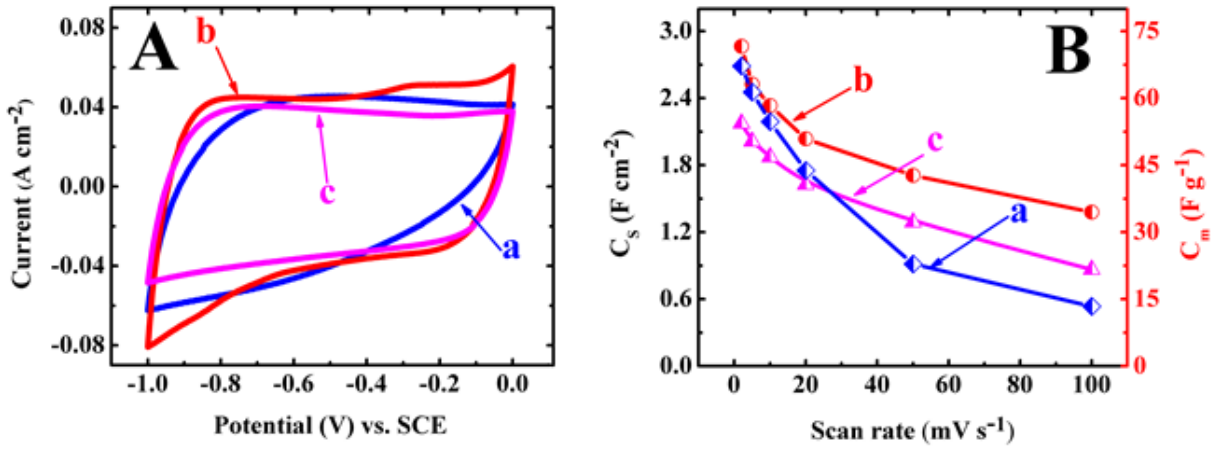

Figure S6. (A) Cyclic voltammograms at a scan rate of 20 mV s^{-1} and (B) specific capacitances versus scan rate for (a) pure AC without CB, and composite electrodes, containing (b) 90% AC and 10% CB (c) 85% AC and 15% CB in 0.5M aqueous Na_2SO_4 electrolyte.

.

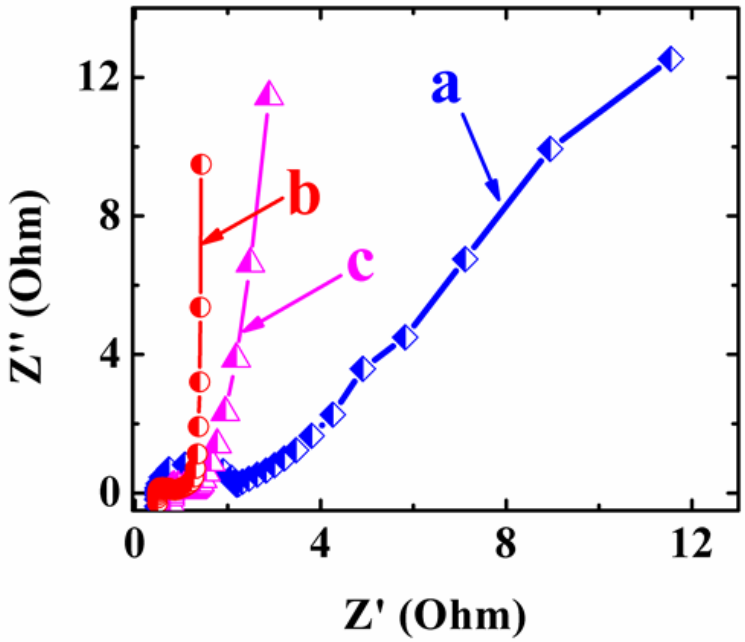

Figure S7. Nyquist plot of complex impedance for (a) pure PICA without CB and composite electrodes, containing (b) 90% AC and 10% CB (c) 85% AC and 15% CB in 0.5M aqueous Na_2SO_4 electrolyte.

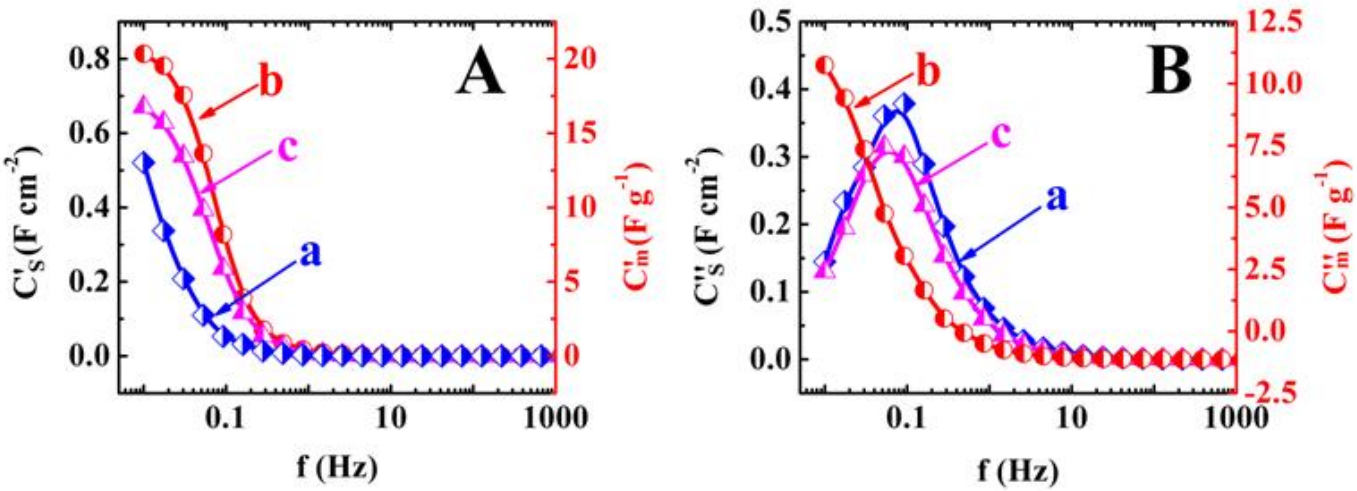

Figure S8. Frequency dependences of components of complex capacitance, calculated from the impedance data (A) C' and (B) C'' for (a) pure AC without CB, and composites , containing (b) 90% AC and 10% CB (c) 85% AC and 15% CB.

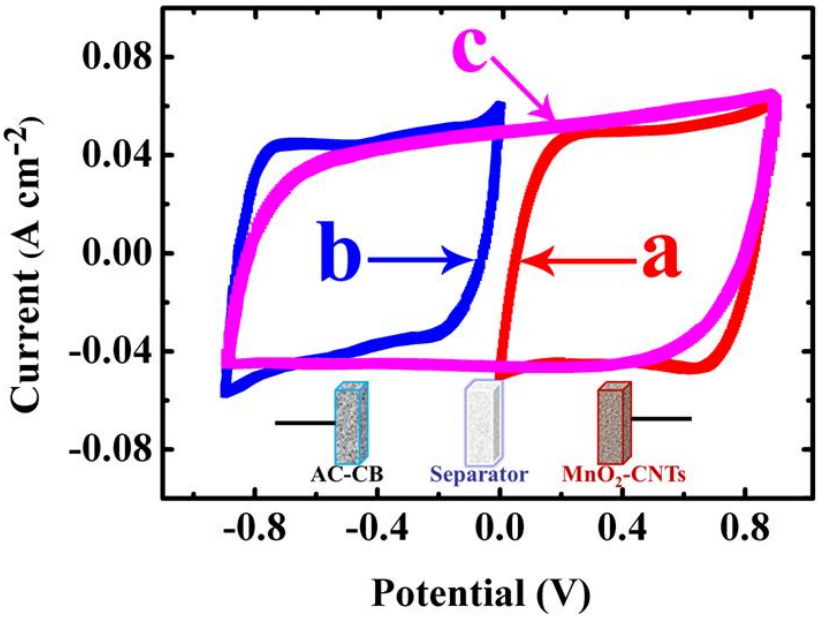

Figure S9. Cyclic voltammograms of (a) MnO_2-MWCNTs composite electrode, (b) AC-CB composite electrode and (c) the cell composed by the two electrodes above at scan rate of 20 mV s^{-1} in 0.5M aqueous Na_2SO_4 electrolyte. The inset shows configuration of the device.